



# Environmental control on the occurrence of high-coercivity magnetic minerals and formation of iron sulfides in a 640 ka sediment sequence from Lake Ohrid (Balkans)

Janna Just<sup>1,2</sup>, Norbert R. Nowaczyk<sup>3</sup>, Leonardo Sagnotti<sup>4</sup>, Alexander Francke<sup>1</sup>, Hendrik Vogel<sup>5</sup>, Jack H. Lacey<sup>6</sup>, and Bernd Wagner<sup>1,2</sup>

<sup>1</sup>Institute of Geology and Mineralogy, University of Cologne, Cologne, Germany

<sup>2</sup>Collaborative Research Centre 806 – Our Way to Europe, University of Cologne, Cologne, Germany

<sup>3</sup>Helmholtz Centre Potsdam, GFZ German Research Centre for Geosciences, Potsdam, Germany

<sup>4</sup>Istituto Nazionale di Geofisica e Vulcanologia, Rome, Italy

<sup>5</sup>Institute of Geological Sciences & Oeschger Centre for Climate Change Research, University of Bern, Bern, Switzerland

<sup>6</sup>NERC Isotope Geosciences Facilities, British Geological Survey, Nottingham, UK

Correspondence to: Janna Just (janna.just@uni-koeln.de)

Received: 31 July 2015 – Published in Biogeosciences Discuss.: 28 August 2015

Revised: 25 January 2016 – Accepted: 8 February 2016 – Published: 8 April 2016

**Abstract.** The bulk magnetic mineral record from Lake Ohrid, spanning the past 637 kyr, reflects large-scale shifts in hydrological conditions, and, superimposed, a strong signal of environmental conditions on glacial–interglacial and millennial timescales. A shift in the formation of early diagenetic ferrimagnetic iron sulfides to siderites is observed around 320 ka. This change is probably associated with variable availability of sulfide in the pore water. We propose that sulfate concentrations were significantly higher before ~ 320 ka, due to either a higher sulfate flux or lower dilution of lake sulfate due to a smaller water volume. Diagenetic iron minerals appear more abundant during glacials, which are generally characterized by higher Fe / Ca ratios in the sediments.

While in the lower part of the core the ferrimagnetic sulfide signal overprints the primary detrital magnetic signal, the upper part of the core is dominated by variable proportions of high- to low-coercivity iron oxides. Glacial sediments are characterized by high concentration of high-coercivity magnetic minerals (hematite, goethite), which relate to enhanced erosion of soils that had formed during preceding interglacials. Superimposed on the glacial–interglacial behavior are millennial-scale oscillations in the magnetic mineral composition that parallel variations in summer insola-

tion. Like the processes on glacial–interglacial timescales, low summer insolation and a retreat in vegetation resulted in enhanced erosion of soil material. Our study highlights that rock-magnetic studies, in concert with geochemical and sedimentological investigations, provide a multi-level contribution to environmental reconstructions, since the magnetic properties can mirror both environmental conditions on land and intra-lake processes.

## 1 Introduction

Rock-magnetic properties of sediments can be used to reveal changing input of the lithogenic fraction and can therefore serve as records of past environmental change. Variations in the concentration of magnetic minerals provide information on changing export of terrigenous sediments from land (DeMenocal et al., 1991; Just et al., 2012; Maher, 2011; Reynolds and King, 1995). Furthermore, variations in the composition of the magnetic mineral assemblages can be used for detecting changes in terrestrial climatic conditions, e.g., weathering and soil formation (Hu et al., 2015; Kämpf and Schwertmann, 1983; Larrasoaña et al., 2015; Lyons et

al., 2010; Maher and Thompson, 1992). However, in addition to the detrital magnetic inventory, magnetic minerals form in the course of syn- and post-sedimentary processes. Magnetotactic bacteria living in the oxic–anoxic transition zone in the topmost sediments utilize magnetic minerals, and can produce either magnetite or greigite intracellularly (Egli, 2004b; Roberts et al., 2012; Snowball et al., 2002; Vali et al., 1989). Furthermore, iron-reducing bacteria may induce the authigenic precipitation of magnetite (e.g., Bell et al., 1987; Frankel and Bazylinski, 2003). On the other hand, the primary magnetic mineral assemblage of detrital origin is often overprinted by post-depositional alteration (Hounslow and Maher, 1999; Nowaczyk et al., 2013; Roberts et al., 1996). The latter results from changing redox conditions at the lake/sea floor and in subsurface sediments leading to dissolution of iron oxides and formation of ferrimagnetic iron sulfides, such as greigite and pyrrhotite (Demory et al., 2005; Froelich et al., 1979; Karlin and Levi, 1983; Rowan et al., 2009; Sagnotti, 2007; Vasiliev et al., 2007) or paramagnetic minerals, such as pyrite, siderite, and vivianite (Dong et al., 2000; Karlin and Levi, 1983).

In addition to the vast number of studies on magnetic minerals in marine sediments, lake sediments can provide valuable information on terrestrial and lacustrine environmental conditions (e.g., Frank et al., 2002; Nowaczyk et al., 2002; Peck et al., 1994, 2004; Roberts et al., 1996; Snowball, 1993; Snowball et al., 1999; Wang et al., 2008). Depending on the trophic state of the lake, water depth, and stratification, oxygen supply is often limited and may lead to excessive dissolution of iron oxides (e.g., Demory et al., 2005; Frank et al., 2013; Nowaczyk et al., 2013; Snowball et al., 1999). In the course of early diagenesis, sulfate is reduced during the process of organic matter degradation in the sulfidic zone (Froelich et al., 1979).  $\text{H}_2\text{S}$  species can react with accessible iron and form iron sulfides. Among them, pyrrhotite and greigite are particularly important for rock and paleomagnetic studies (Roberts et al., 2011a; Sagnotti, 2007). As these secondary magnetic iron minerals acquire a remanent magnetization iron sulfides can bias the primary magnetic signals (Ron et al., 2007), in general carried by detrital (titanio)magnetite. Although pyrrhotite and greigite may form as early diagenetic metastable phases during the chemical reaction pathway to pyrite, studies have shown that they may be preserved if the concentration of organic matter, and consequently organic-bound sulfur, is low and pyritization is hampered by Fe excess (Blanchet et al., 2009; Kao et al., 2004; Roberts et al., 1996; Skinner et al., 1964). Cyclic preservation of greigite in a Pliocene lacustrine sequence from Lake Qinghai (China) was recently linked to periods of high lake levels and humid climate that resulted in oxygen depletion of the bottom water (Fu et al., 2015).

Compared to the ocean, lakes generally contain lower sulfate concentrations, and therefore sulfate may be exhausted at shallow depths in the sediment or even in the water column. Below the sulfidic zone, methanogenesis is the most impor-

tant process for the degradation of reactive organic matter (Capone and Kiene, 1988; Roberts, 2015). Here, Fe species may react to form iron phosphate (vivianite) or iron carbonate (siderite; Berner, 1981; Roberts, 2015). In addition to the “early” diagenetic processes, concurring with organic matter degradation, authigenic Fe minerals can form at a late diagenetic phase. Such precipitation and dissolution processes occur mainly as a result of a variety of different mechanisms associated with the migration of mineralized fluids and with changes in the pore water chemistry, which disrupt the steady-state diagenetic progression (Roberts and Weaver, 2005; Sagnotti et al., 2005).

Because of the imprint of these interacting processes, rock-magnetic properties of lake sediments can provide a suite of environmental information. These range from variations in the external supply of magnetic detrital mineral phases to changes in lake water oxygenation and sulfate supply and in conditions favorable for magnetotactic bacteria. The sediments from Lake Ohrid on the Balkan Peninsula (Fig. 1) provide an excellent opportunity to study these processes over several glacial–interglacial cycles. Lake Ohrid is the oldest lake in Europe, dating back to  $>1.2$  Ma (Wagner et al., 2014). Its sediments consist of lacustrine carbonates (mostly calcite), biogenic silica, and lithogenic compounds (Francke et al., 2015). Lake Ohrid is an oligotrophic lake; a complete overturn and deep mixing occur only every few years, while the upper 200 m of the water column is mixed every year during winter (e.g., Matzinger et al., 2007). Temperature variations probably had a strong influence on shallow and deep mixing of Lake Ohrid during past glacials and interglacials (Vogel et al., 2010a; Wagner et al., 2009); however, to date there is no quantitative estimate of this effect.

Terrestrial element concentrations and gamma ray intensities of Lake Ohrid sediments mirror phases of enhanced erosion in the catchment on glacial–interglacial timescales (Baumgarten et al., 2015; Francke et al., 2015). Geochemical variations in a core from northeastern Lake Ohrid (Fig. 1) are indicative of changes in sediment dynamics over the last  $\sim 140$  kyr. Here, the increasing deposition of Cr-rich minerals, most likely originating from the western flanks of Lake Ohrid, are thought to result from either enhanced erosion of soils or stronger wind activity, inducing changes in surface water circulation (Vogel et al., 2010a).

This first study on the magnetic properties of the Lake Ohrid “DEEP” Site (ICDP 5045-1) focusses on observations of changing magnetic mineralogy and possible implications for lacustrine and terrestrial environmental conditions. We aim to identify primary detrital magnetic minerals, and evaluate whether these reveal changing environmental conditions in the catchment, beyond the observed general pattern of higher (lower) terrigenous input during glacials (interglacials). Secondly, we discuss the occurrence of (early) diagenetic minerals to develop a working hypothesis concerning changes in redox conditions and shifts in the chemical and hydrological environment in the lake. To address these

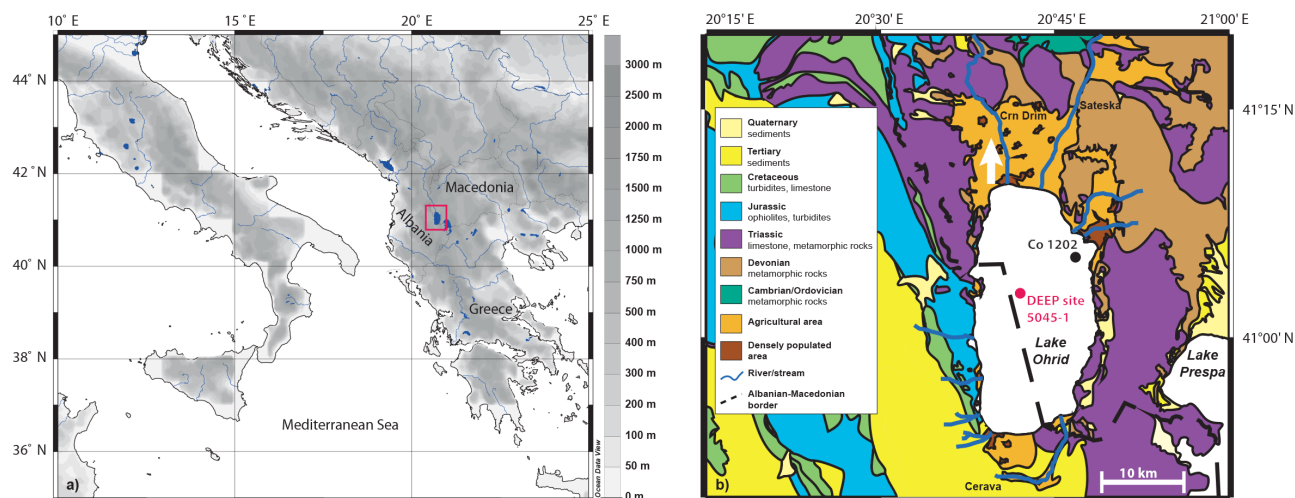


**Figure 1.** (a) Overview map of the Balkan Peninsula. (b) Geological map of the Lake Ohrid region and coring locations of the DEEP site (5045-1) and Co1202 (Vogel et al., 2010a). Modified after Vogel et al. (2010b).

objectives, we jointly investigated mineral magnetic properties and organic proxies, X-ray fluorescence (XRF) data (Francke et al., 2015) and Fourier transform infrared spectroscopy (FTIRS; Lacey et al., 2016).

## 2 Study area and materials

Lake Ohrid (45°54'N, 38°20'E; Fig. 1) is located at the boundary between Albania and the Former Yugoslav Republic of Macedonia at an altitude of 690 m above sea level. It is ~30 km long and ~15 km wide, and has a maximum water depth of 293 m. It is flanked by high mountain ranges in the west (Jurassic ophiolites and Triassic carbonates) and east (Triassic carbonates), and an alluvial plain in the north (Fig. 1, Hoffmann et al., 2010, and references therein; Vogel et al., 2010b). Modern vegetation is dominated by deciduous forest (Lézine et al., 2010).

At present, there are two major rivers draining into Lake Ohrid, the Sateska in the north and Cerava in the south, bringing detrital sediments to the lake. Freshwater is supplied to the lake by rivers (25 %), direct precipitation (25 %) and karst aquifers (50 %). The karst aquifers are fed by mountain range precipitation and from the neighboring higher-altitude (849 m above sea level) Lake Prespa. The gain in fresh water is balanced by the drainage through the river Crn Drim (accounting for 60 % of water loss) and evaporation (~40 %) of lake water (Matzinger et al., 2006a, b; Wagner et al., 2014).

Maximum precipitation occurs during winter, and air temperatures at present range between -5 and 31 °C (Popovska and Bonacci, 2007). Ohrid is an oligotrophic lake with maximum productivity during summer (Matzinger et al., 2007; Wagner et al., 2010). However, at present, it shows indications for the onset of eutrophication (e.g., Matzinger et al., 2007).

Six holes were drilled at the “DEEP” site (ICDP Site 5045-1) as part of the SCOPSCO project (Scientific Collaboration on Past Speciation Conditions in Lake Ohrid) in summer 2013 down to a maximum sediment penetration of 569 m (Fig. 1b). The recovered sedimentary sequence is thought to cover more than 1.2 Myr (Wagner et al., 2014). A composite profile was constructed and an age model was developed by Francke et al. (2015) which is based on 11 tephrostratigraphic tie points (Leicher et al., 2015) and correlating geochemical proxies to orbital parameters (using an age uncertainty of ±2000 years). Here, we analyzed the upper 247 m of the composite profile. The age model reveals that the analyzed interval spans the past 637 kyr.

## 3 Methods

### 3.1 Rock-magnetic measurements

We sampled the composite profile at 50 cm (0–100 m) and 48 cm (100–247 m) intervals – in total 500 samples – using 6.2 cm<sup>3</sup> oriented plastic boxes. Magnetic susceptibility  $\chi$  was measured using an AGICO MFK-1 susceptometer. Natural and artificial remanence parameters were measured using a 2G Enterprises 755 superconducting long-core rock magnetometer with an in-line tri-axial alternating field (AF) demagnetizer. The natural remanent magnetization (NRM) was demagnetized in 10 incremental steps of up to 100 mT AF peak amplitude. Anhyseretic remanent magnetization (ARM), a proxy for fine-grained, mostly single domain (SD) and pseudosingle domain (PSD) magnetite (King et al., 1982), was imparted with a single-axis 2G 600 AF demagnetizer by using 100 mT AF and 50  $\mu$ T DC field. Subsequently, ARM was AF-demagnetized at fields of 10, 20, 30, 40, 50, and 65 mT. The median destructive field

( $MDF_{ARM}$ ), defined as the field required to decrease ARM by 50 %, was calculated. This parameter is indicative of the coercivity within the fine ferrimagnetic mineral fraction.

Isothermal remanent magnetization (IRM), which depends on the magnetic mineral mixture in the samples, was induced using a 2G 660 pulse magnetizer applying a 1500 mT DC peak field and a 200 mT reversed field. The ratio of  $\chi_{ARM}$  to saturation IRM ( $\chi_{ARM} / SIRM$ ) serves as a proxy for the magnetic grain size. Furthermore, hard IRM (HIRM), reflecting the contribution of high-coercivity magnetic minerals to SIRM, was calculated using the equation

$$HIRM = 0.5(SIRM + IRM_{(-200\text{mT})}). \quad (1)$$

Additionally, the  $S$  ratio, calculated as

$$S = 0.5 \times (1 - (IRM_{(-200\text{mT})} / SIRM)), \quad (2)$$

serves as a proxy for the proportion of high- (e.g., hematite + goethite,  $0 < S < 1$ ) to low-coercivity (magnetite, greigite) magnetic minerals ( $0 < S < 1$ ).

Moreover, we calculated  $SIRM / \chi$ , which is often observed to be elevated in the presence of greigite (e.g., Maher and Thompson, 1999; Nowaczyk et al., 2012; Snowball and Thompson, 1990). Another characteristic behavior of greigite is that it acquires a so-called gyro-remanent magnetization (GRM). To further quantify the possible imprint of greigite, we calculated the ratio between the differences of final remanent magnetization (FRM) at 100 mT AF peak amplitude and minimum magnetization (MRM) during NRM demagnetization, and the difference of NRM and MRM according to (Fu et al., 2008)

$$\Delta GRM / \Delta NRM = (FRM - MRM) / (NRM - MRM). \quad (3)$$

To account for down-core increasing sediment compaction, magnetic concentration parameters were mass-normalized using the dry bulk density. The latter data were available at 4 cm intervals and interpolated to the depths of magnetic samples.

### 3.2 Cluster analysis

We performed fuzzy c-means cluster analysis for a suite of data that are indicative of the magnetic mineralogy and magnetic granulometry. To achieve symmetric distributions of the suite of data, we performed data  $\ln$  (natural logarithm) transformations, except for  $\Delta GRM / \Delta NRM$  and the  $S$  ratio. The latter parameters show a  $J$ -shaped distribution that cannot be transformed into a normal distribution. All data sets were standardized before clustering.

### 3.3 Scanning electron microscopy of magnetic extracts

Six samples that are characterized by divergent magnetic properties were selected for scanning electron microscopy (SEM) analyses. Magnetic extracts were prepared following

the protocol of Nowaczyk (2011). A total of 2 cm<sup>3</sup> of sediment was dispersed in 60 mL of alcohol and Na solution was added. The solutions were put in an ultrasonic bath for 10 min. A rare-earth magnet inside a plastic hose was submerged into the solution. Minerals attracted to the hose were washed into a fresh vial. The procedure was repeated twice to obtain a clean extract. Particles in the alcohol solution were then concentrated and a drop of the solute was placed on an SEM stub and sputtered with carbon.

Magnetic extracts were analyzed using a Carl Zeiss SMT Ultra 55 Plus SEM. Images were obtained using the secondary and back scatter electron beams of single particles. To obtain the chemical composition of the analyzed particles, energy dispersive spectroscopy was performed at energy levels of 20 keV.

### 3.4 Geochemical and mineralogical data

Total organic carbon (TOC), total inorganic carbon (TIC) and X-ray fluorescence (XRF) data, measured by Francke et al. (2015), are used for discussion of rock-magnetic data. XRF scanning was carried out at 2.5 mm resolution and with an integration time of 10 s using an ITRAX core scanner equipped with a chromium X-ray source. Total carbon (TC) and total TIC were analyzed at 16 cm resolution. For TIC, homogenized and dispersed sediments were treated with phosphoric acid. TC and TIC was measured in the form of released CO<sub>2</sub> after combustion at 900 and 160 °C, respectively, using a DIMATOC 100. Total organic carbon (TOC) content was calculated from the mass difference between TC and TIC. In addition, we show relative changes in siderite (FeCO<sub>3</sub>) concentration determined from infrared (IR) spectra. IR spectra were measured on a Bruker Vertex 70 Fourier transform infrared (FTIR) spectrometer at the Institute of Geological Sciences at the University of Bern. Details on measurement set up and data evaluation procedures are outlined in Lacey et al. (2016).

## 4 Results

### 4.1 Rock magnetism

In the magnetic properties, a major change is visible around ca. 320 ka corresponding to the transition between Marine Isotope Stage (MIS) 9 and MIS 8. Below this transition the  $S$  ratio is rather constant but SIRM shows large amplitudinal change, while above the transition SIRM is relatively constant but compositional magnetic proxies, e.g. the  $S$  ratio, show interglacial–glacial variability. We therefore divided the record into two magnetic units (Fig. 2).

### 4.2 MIS 16–MIS 9 (unit 2)

Except for a stable  $S$  ratio (Fig. 2e), this unit is characterized by high-amplitude variations on glacial–interglacial

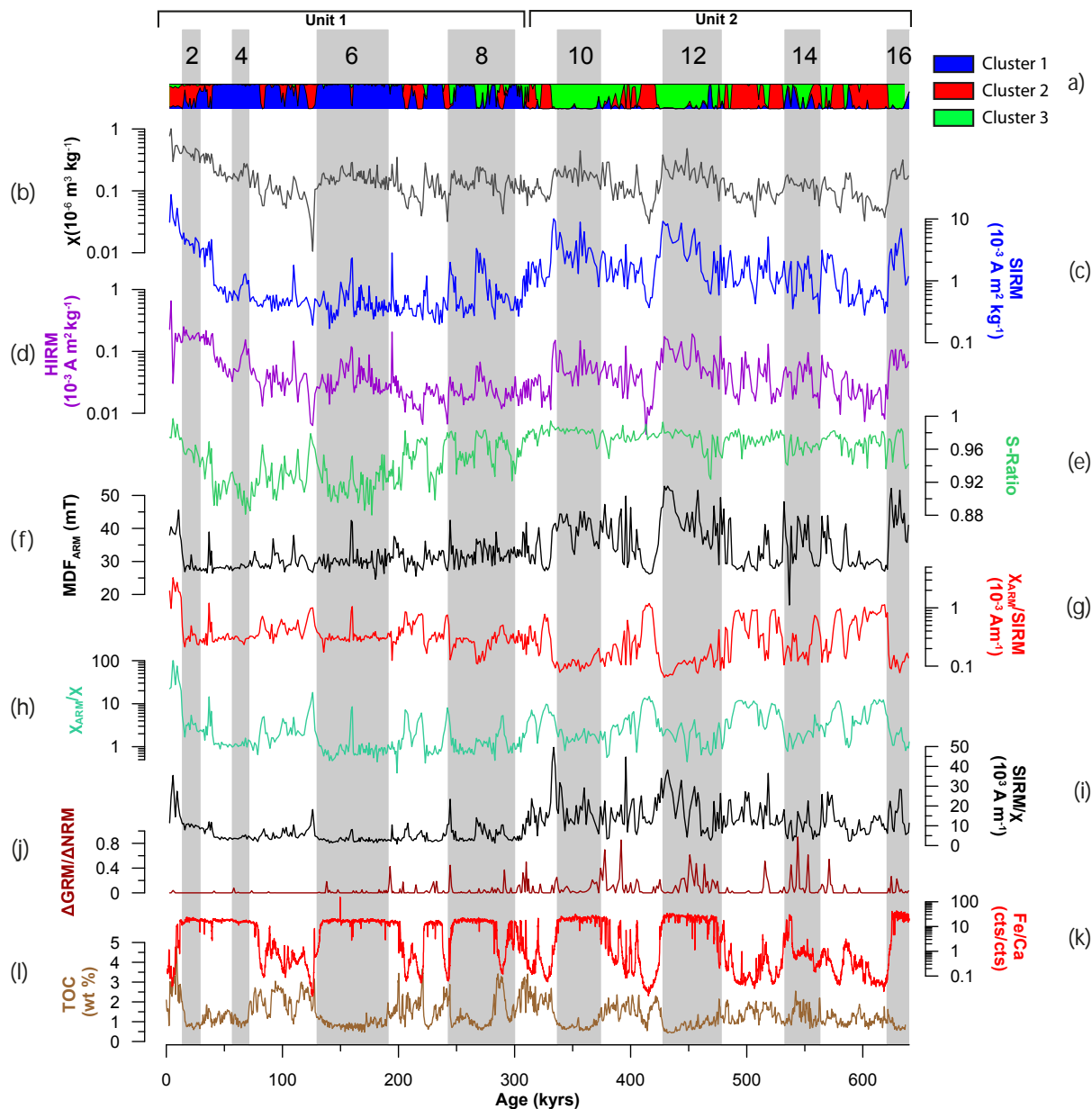


**Figure 2.** Compilation of magnetic and geochemical parameters measured on samples from the DEEP site. (a) Color bar indicates cluster-membership coefficients for each sample corresponding clusters in Table 2. (d–j) Rock-magnetic proxies; for abbreviations see text. (k) XRF scanning Fe/Ca counts. TOC concentrations (l) are from Francke et al. (2015). Gray bars represent marine oxygen isotope stages after Lisiecki and Raymo (2005).

timescales. Susceptibility (Fig. 2b) and SIRM (Fig. 2c) and HIRM (Fig. 2d) are elevated during glacials, while  $\chi_{ARM}/SIRM$  (Fig. 2g) and  $\chi_{ARM}/\chi$  (Fig. 2h) decrease and the  $MDF_{ARM}$  (Fig. 2f) rises to fields of up to 50 mT. Increasing  $\Delta GRM/\Delta NRM$  (Fig. 2j) is often associated with interglacial–glacial transitions, as well as early glacials. Moreover, short-lasting spikes of GRM acquisition during interglacials are accompanied by brief increases in Fe/Ca ratios (Fig. 2k, e.g., during MIS 15, 13, 11). In contrast,

$SIRM/\chi$  (Fig. 2i) shows maximum values at the end of the glacials (MIS10, MIS12), when GRM acquisition is mostly low.

#### 4.3 MIS 8–MIS 1 (unit 1)

Compared to unit 2, glacial–interglacial variations are expressed through different proxies.  $SIRM/\chi$  (Fig. 2i) is low and  $\Delta GRM/\Delta NRM$  (Fig. 2j) is mostly zero. SIRM (Fig. 2c) and the  $MDF_{ARM}$  (Fig. 2f) are relatively stable, while sus-

ceptibility (Fig. 2b) and HIRM (Fig. 2d) show glacial–interglacial cyclicity.  $\chi_{\text{ARM}}/\text{SIRM}$  (Fig. 2g),  $\chi_{\text{ARM}}/\chi$  (Fig. 2h) and the  $S$  ratio (Fig. 2e) is lower during glacials, in concert with higher TOC (Fig. 2l) and lower Fe/Ca ratios (Fig. 2k). An exception to this glacial–interglacial behavior is observed in the uppermost part of unit 1, where TOC increases and Fe/Ca decreases. In contrast to the relationship observed for the rest of the unit, the intensity of the magnetic concentration parameters ( $\chi$  SIRM, Fig. 2b, c) increases, and the  $S$  ratio rises to high values. Also, the  $\text{MDF}_{\text{ARM}}$  and  $\chi_{\text{ARM}}/\text{SIRM}$  and  $\chi_{\text{ARM}}/\chi$  and  $\text{SIRM}/\chi$  rise to maximum values.

#### 4.4 SEM observations

We analyzed samples that are characterized by diverging magnetic properties (see Table 1). Detrital titanomagnetites and chromium iron oxides are present in almost all analyzed samples (Fig. 3a, b, d). Magnetic extracts from the upper unit contain relatively high proportions of siderite (Fig. 3g), whereas iron sulfides are abundant in samples from the lower unit (Fig. 3c–f, h).

All analyzed samples in unit 2 are characterized by a high  $\text{MDF}_{\text{ARM}}$  ( $>45$  mT). Of those, two samples acquired a significant GRM ( $>68\%$ ), but had relatively low  $\text{SIRM}/\chi$ , while the other two samples have the most extreme  $\text{SIRM}/\chi$  and insignificant GRM acquisition (Table 1). The high GRM samples contain mixtures of titanium magnetites and fine-grained and microcrystalline iron sulfides, which most likely correspond to greigite (Fig. 3c, d). Also, the low GRM samples contained fine-grained iron sulfides and idiomorphic greigite crystals but, additionally, large iron sulfide nodules (Fig. 3e, f, h) that apparently have a higher Fe:S ratio compared to the finer-grained greigite (data not shown). Although the number of investigated SEM samples is relatively low, the results suggest that a high  $\text{MDF}_{\text{ARM}}$  appears closely related to or at least accompanied by the general presence of iron sulfides, while maximum  $\text{SIRM}/\chi$  is associated with the coarse-grained sulfide nodules. GRM is quite strong when microcrystalline or individual greigite crystals occur.

## 5 Discussion

### 5.1 Magnetic proxy evaluation

Many samples from unit 2 have high values in  $\text{MDF}_{\text{ARM}}$ ,  $\text{SIRM}/\chi$  and  $\Delta\text{GRM}/\Delta\text{NRM}$  (Fig. 2f, i, j), which are often associated with the presence of greigite (e.g., Fu et al., 2008; Peters and Dekkers, 2003; Rowan et al., 2009). It is important to note that these parameters can sometimes provide ambiguous results; high  $\text{SIRM}/\chi$  is not always accompanied by high  $\Delta\text{GRM}/\Delta\text{NRM}$ ; however,  $\text{MDF}$ s are high if any of the former proxies are elevated. Missing GRM acquisition of greigite bearing samples has been reported in other studies (Roberts et al., 1998; Sagnotti et al., 2005), and could

be related to grain-size effects, because only fine-grained (SD) greigite acquires GRM. As observed in the images of the magnetic extracts, coarse-grained iron sulfides are abundant in samples with low GRM and high  $\text{SIRM}/\chi$  and we therefore hypothesize that greigite either grew to too coarse grain size for GRM acquisition or was transformed into other iron sulfides, e.g., pyrrhotite, which is also characterized by high  $\text{SIRM}/\chi$  (Maher and Thompson, 1999). Variations on interglacial–glacial timescales within the upper unit are the second significant feature in the rock-magnetic record. The variations could stem from compositional changes in the magnetic mineral supply to the lake, but they could also result from selective dissolution of low-coercivity magnetic minerals. To further evaluate the rock-magnetic properties, we show cross plots of selected parameters (Fig. 4). As  $\Delta\text{GRM}/\Delta\text{NRM}$  is a robust indicator for the presence of greigite, the cross plot is color-coded according to GRM acquisition.

The  $\chi_{\text{ARM}}/\text{SIRM}$  ratio (Fig. 2g) is often utilized as a proxy for magnetic grain size, but it can be biased if SIRM is dominated by high-coercivity magnetic minerals (HIRM). However, HIRM is more than 2 orders of magnitude smaller than SIRM (Fig. 2), and thus SIRM can be applied as a proxy for the concentration of the low-coercivity fractions (e.g., magnetite and greigite).

For non-GRM samples, low  $S$  ratios are associated with low  $\chi_{\text{ARM}}/\text{SIRM}$  (Fig. 4a), implying that a shift towards high-coercivity minerals is accompanied by a coarsening of the low-coercivity fraction. In contrast, GRM samples have high  $S$  ratios but low  $\chi_{\text{ARM}}/\text{SIRM}$  values, indicating that in combination these parameters are valuable indicators for the presence of greigite. The low  $\chi_{\text{ARM}}/\text{SIRM}$  ( $0.06\text{--}0.2 \times 10^{-3} \text{ mA}^{-1}$ ) values of the latter samples lie close to the range of authigenic inorganically precipitated greigite which is characterized by  $0.058\text{--}0.084 \times 10^{-3} \text{ mA}^{-1}$  (Snowball, 1997a), in contrast to high values observed for sediments containing bacterial magnetite (Snowball, 1994) and greigite (Reinholdsson et al., 2013, Fig. 3b). Only a few samples that did not acquire GRM lie in these latter areas, i.e., samples from the uppermost part of the core (cf. Fig. 2g, h). These results suggest that except for the latter samples, a significant contribution of magnetite and greigite magnetosomes can be ruled out as a source for rock-magnetic signals. Furthermore, we propose that greigite, within the GRM acquiring samples, formed out of a chemical process. However, this process was likely induced by biological activity (iron-reducing bacteria).

There appears to be a strong positive correlation between  $\text{SIRM}/\chi$  and  $\chi_{\text{ARM}}/\chi$  (Fig. 4c). The latter parameter is often used as a magnetic grain-size indicator for low-coercivity minerals, especially magnetite, while  $\text{SIRM}/\chi$  can be influenced by different mechanisms, ranging from changes in magnetic grain size (Peters and Dekkers, 2003) and magnetic mineralogy, including the presence of greigite (Frank et al., 2007; Fu et al., 2008; Nowaczyk et al., 2012; Reinholdsson et

**Table 1.** Magnetic properties of samples used for scanning electron microscopy.

Depth (m)	Age (kyr)	MDF (mT)	SIRM/ $\chi$ ( $10^3 \text{ A m}^{-1}$ )	$\Delta\text{GRM}/\Delta\text{NRM}$	$\chi_{\text{ARM}}/\text{SIRM}$ ( $10^{-3} \text{ m A}^{-1}$ )	Observations	Fig. 3
10.53	26	27	9.8	0.00	0.24	Ti magnetite, magnetite Cr-Fe oxide, Mg-Cr spinel, Fe-Mn oxide	b
72.53	177	33	3.0	0.00	0.31	Ti magnetite, magnetite Cr-Fe oxide, Mg-Cr spinel, Fe-Mn oxide, siderite	a
117.83	270	36	11.6	0.00	0.12	siderite, Fe-S nodules	g
153.83	360	45	29.1	0.01	0.09	(microcrystalline) Fe sulfide aggregates, idiomorphic greigite, siderite, Ti magnetite	e, f
158.63	378	47	22.5	0.70	0.10	fine-grained Fe-S (greigite?), Ti magnetite, Cr-Fe oxide	c
162.47	392	46	20.6	0.85	0.11	fine-grained Fe-S (greigite?), Ti magnetite	d
176.87	432	53	38.2	0.01	0.07	coarse-grained Fe-S nodules, fine-grained greigite	h

al., 2013; Snowball, 1997b). Although paramagnetic minerals may contribute to the susceptibility, this bias would be expressed in both ratios, and a cross plot of those two parameters is valid to compare ferrimagnetic mineralogical properties between samples. The linear behavior of the two parameters indicates that SIRM/ $\chi$  is influenced by magnetic grain-size effects. However, the bigger gradient for GRM samples implies that the presence of greigite is shifting SIRM to higher levels.

The  $\text{MDF}_{\text{ARM}}$  is indicative of the hardness of magnetic minerals within the low-coercivity magnetic fraction (i.e. SD and PSD magnetite), and is therefore also affected by a preferential dissolution of fine magnetic particles. As outlined above, the  $S$  ratio signifies the relative concentration of high- vs. low-coercivity minerals and is influenced by relative increases in high-coercivity particles, or decreases in magnetite, the latter could also be induced by dissolution. From the MDF and  $S$  ratio plot, two clusters can be distinguished (Fig. 4d). Non-GRM samples have MDFs between 25 and 33 mT and a broad range of  $S$  ratios, whereas the MDF for GRM samples is higher than 30 mT and are mainly confined by  $S$  ratios higher than 0.96. The co-occurrence of high MDFs and GRM acquisition strongly suggests that increasing coercivity results from the presence of greigite. Moreover, the high  $S$  ratios reveal that greigite mostly contributes to the low-coercivity component of magnetization. For the non-GRM samples the pattern implies that relative increases of the high-coercivity fraction are not accompanied by changes within the low-coercivity mineral assemblage. A preferential dissolution of ferrimagnetic minerals, expressed as a drop in the  $S$ -Ratio, would be expected to be accompanied by changing coercivity also within low-coercivity assemblage (i.e., changing MDF). This is not observed for our samples. Moreover, the constant SIRM throughout unit 1, whereby HIRM shows variations (cf. Fig. 2c, d), rather indicates the addition of high-coercivity minerals, instead of a decrease in low-coercivity minerals. Further support for this

hypothesis comes from the low TOC concentrations accompanying the low  $S$  ratio intervals. Enhanced magnetite dissolution is typically observed when TOC concentrations are elevated. The trend in the magnetic proxies, however, shows the opposite of what would be expected in the case of enhanced dissolution. The  $S$  ratio indicates even higher contents of low vs. high-coercivity minerals during interglacials with elevated TOC content. We therefore assume that, if reductive diagenesis had occurred, it affected the whole unit equally, and variation in the  $S$  ratio is indicative of increasing high-coercivity minerals within the detrital magnetic mineral fraction.

We also conducted high-temperature susceptibility measurements, in order to discriminate the iron sulfides. The susceptibility of all samples increased sharply above 400 °C and decreased above 500 °C (data not shown). The cooling curve has higher susceptibilities. This behavior is typical if reduced iron is oxidized to magnetite upon heating. This iron, however, can be derived from different mineral phases, e.g., from clay minerals (Bell et al., 1987) or iron sulfides and siderites.

## 5.2 Cluster analysis

To further evaluate temporal changes in the magnetic mineralogy of Lake Ohrid sediments we performed a cluster analysis. Based on the evaluation of the magnetic parameters, we included  $\chi_{\text{ARM}}/\chi$ ,  $\chi_{\text{ARM}}/\text{SIRM}$ ,  $S$  ratio, MDF and  $\Delta\text{GRM}/\Delta\text{NRM}$  which are indicative of magnetic grain size, magnetic coercivity, and the occurrence of greigite.

Cluster center 3 is characterized by the lowest  $\chi_{\text{ARM}}/\text{SIRM}$  value, high  $S$ -Ratio, a high MDF of 40 mT and a high GRM (Table 2). These characteristics are often observed for sediments containing chemically produced greigite (Fig. 4); thus we infer that cluster 3 is related to greigite and other ferrimagnetic iron sulfides, e.g., pyrrhotite.

Cluster centers 1 and 2 have similarly low GRM and MDF, indicating the absence of greigite and undistinguish-

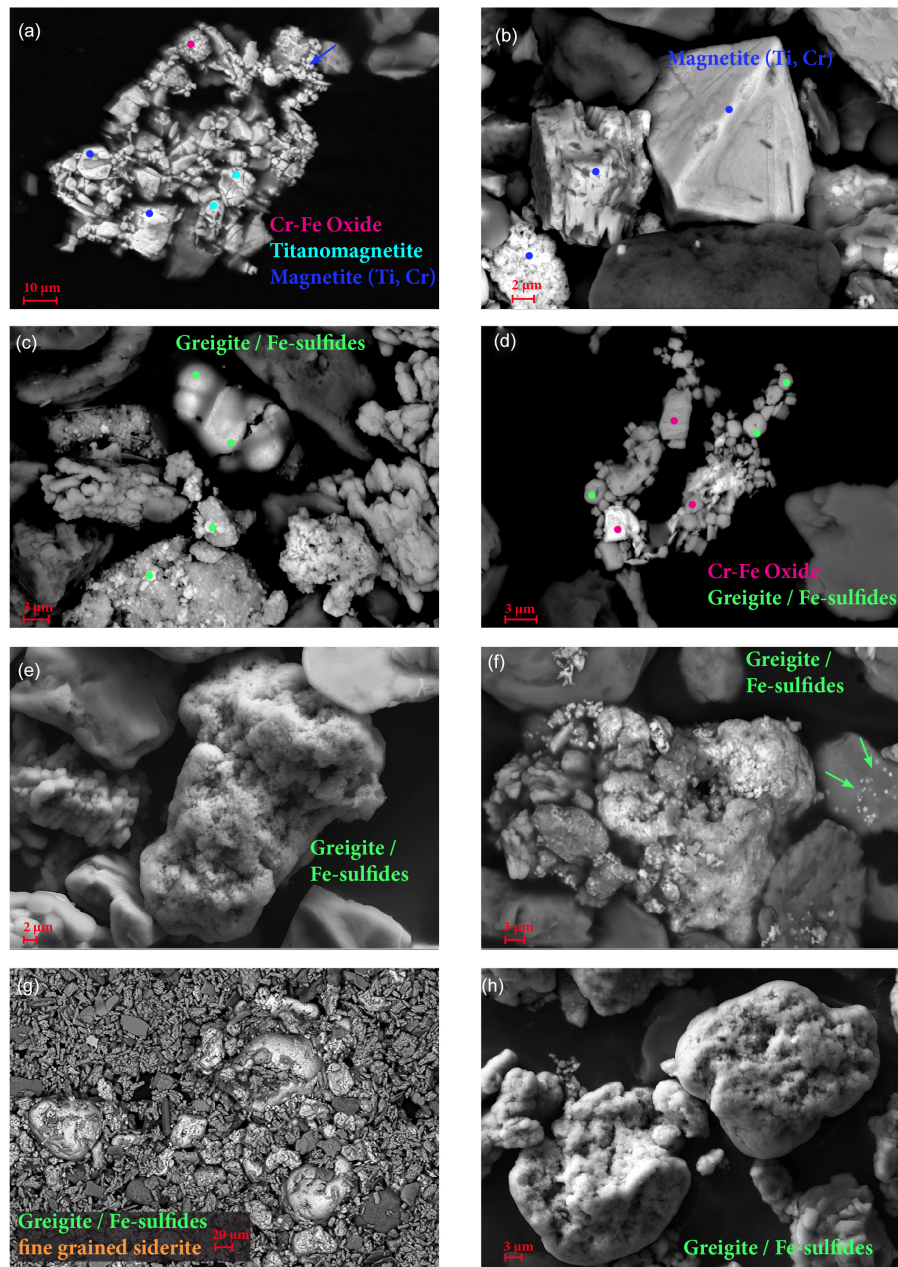


**Figure 3.** SEM images of magnetic extracts; see also Table 1. (a) 72.53 m depth, detrital chromium iron oxides, titanomagnetite and magnetite with traces of Cr and Ti. (b) 10.53 m depth, idiomorphic and fragments of magnetites, traces of Ti and Cr. (c) 158.83 m depth, microcrystalline and framboidal iron sulfides within organic shell. (d) 162.47 m depth, chromium iron oxides, fine-grained greigite aggregates. (e) 153.83 m depth, microcrystalline iron sulfide nodule. (f) 153.83 m depth, microcrystalline iron sulfide aggregates, idiomorphic greigite crystals (arrows). (g) 117.83 m depth, coarse Fe-S nodules and fine-grained siderite grains (elongated particles). (h) 176.87 m depth, microcrystalline iron sulfide nodule.

able different coercivities within the magnetically soft fraction. However,  $\chi_{ARM} / \chi$ ,  $\chi_{ARM} / SIRM$  and the  $S$  ratio are lower in cluster 1 compared to cluster 2. As discussed in Sect. 5.1, the differences are due to the higher contribution of high-coercivity minerals, concurrent with a coarsening of the ferrimagnetic fraction.

The variations in cluster membership coefficients (Fig. 2a) captures the variability in magnetic proxies (Fig. 2b–j). Cluster 1 mainly relates to interglacial samples, whereas cluster 2 corresponds mainly to glacial samples in the upper part of the core (Fig. 5f). Glacial samples from the lower part of the core are associated with cluster 3.

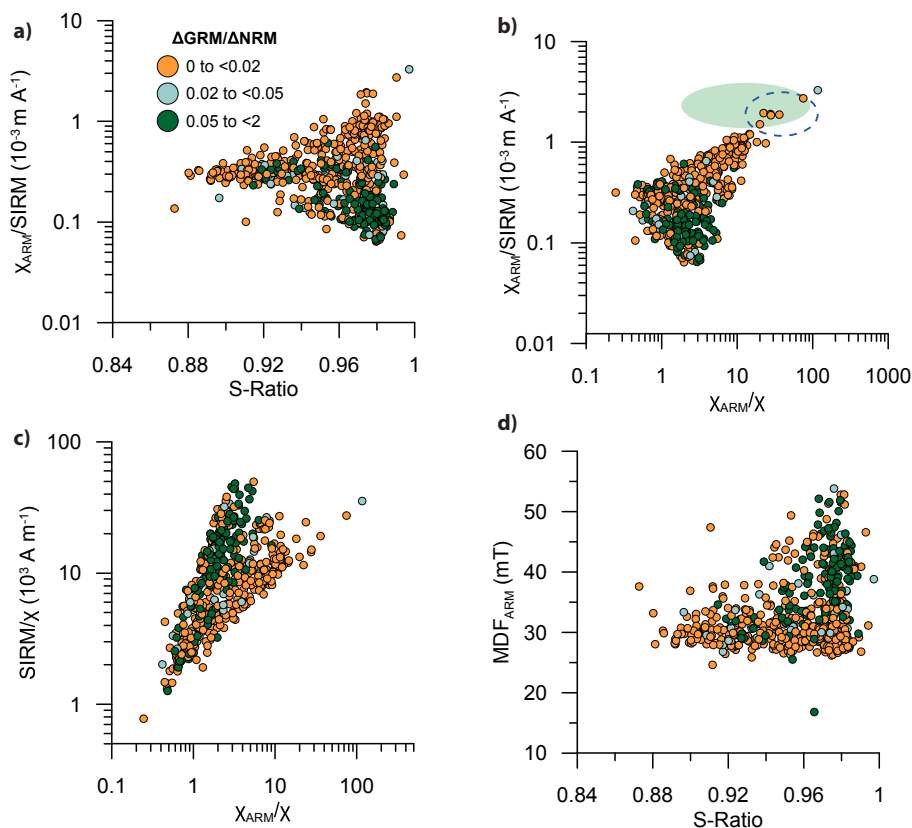


**Figure 4.** Selected cross plots of magnetic proxy evaluation. Samples that acquire GRM (color code) cluster in different regions of the diagrams. **(a)** GRM samples are characterized by high  $S$  ratios. A linear relationship between  $\chi_{\text{ARM}} / \text{SIRM}$  and  $S$  ratio relates to co-varying ferrimagnetic grain-size fining and increasing low- vs. high-coercivity magnetic mineral content. **(b)** GRM samples plot at  $\chi_{\text{ARM}} / \text{SIRM}$  levels typical of authigenic, inorganically precipitated greigite. A few samples from the uppermost part of the core plot in the field of bacterial magnetite (dashed circle; Snowball, 1994) and greigite (green shaded area; Reinholdsson et al., 2013). **(c)** GRM samples have a distinctively different gradient compared to non-GRM samples in the  $\text{SIRM} / \chi$  vs.  $\chi_{\text{ARM}} / \chi$  plot. **(d)** GRM samples are characterized by high  $S$  ratios and high  $\text{MDF}_{\text{ARM}}$ . Non-GRM samples show no relationship between the two parameters.

**Table 2.** Cluster center properties obtained from fuzzy c-means clustering.

	$\chi_{\text{ARM}} / \chi$	$\chi_{\text{ARM}} / \text{SIRM}$ ( $10^{-3} \text{ m A}^{-1}$ )	$S$ ratio	$\text{MDF}_{\text{ARM}}$ (%)	$\Delta \text{GRM} / \Delta \text{NRM}$
Cluster 1	1.10	0.30	0.93	30.69	2.79
Cluster 2	5.53	0.55	0.97	29.85	2.08
Cluster 3	1.89	0.13	0.97	39.86	11.95

### 5.3 Iron sulfides in Lake Ohrid sediments

The concentration of magnetic minerals, approximated by remanence intensities (and susceptibilities), is relatively low in Lake Ohrid sediments in the upper unit. This gives a strong indication that the magnetic fraction was subject to reductive diagenesis. In unit 2, remanence intensities are enhanced, due to the presence of ferrimagnetic iron sulfides (Fig. 2). Concerning the occurrence of greigite and iron sulfides, the cluster analysis reveals two different patterns that modulate each other (Fig. 5f): firstly, the absence of iron sulfides in

unit 1, and secondly, a cyclic occurrence of iron sulfides on glacial–interglacial timescales in unit 2. Besides iron sulfides, siderite, which also forms during (early) diagenesis, is contained in the sediments. When discussing the mechanism for diagenetic iron-mineral formation, it is worthwhile also considering the occurrence of paramagnetic siderites.

### 5.4 Early vs. late diagenetic formation

For iron sulfides to precipitate, accessible Fe and S have to be available. In the course of early diagenesis sulfate is reduced during organic matter degradation. Typically, iron sulfides such as greigite and pyrite form in the sulfidic pore water zone, associated with the upward-migrating sulfate–methane transition zone (SMTZ), where  $\text{H}_2\text{S}$  accumulates (Kasten et al., 1998).

In contrast, siderite mainly forms in the methanogenic zone, if pore waters have high  $\text{CaCO}_3$  concentrations (e.g., Berner, 1981; Roberts, 2015). However, siderite and greigite (iron sulfides) can form at the same time if the rate of

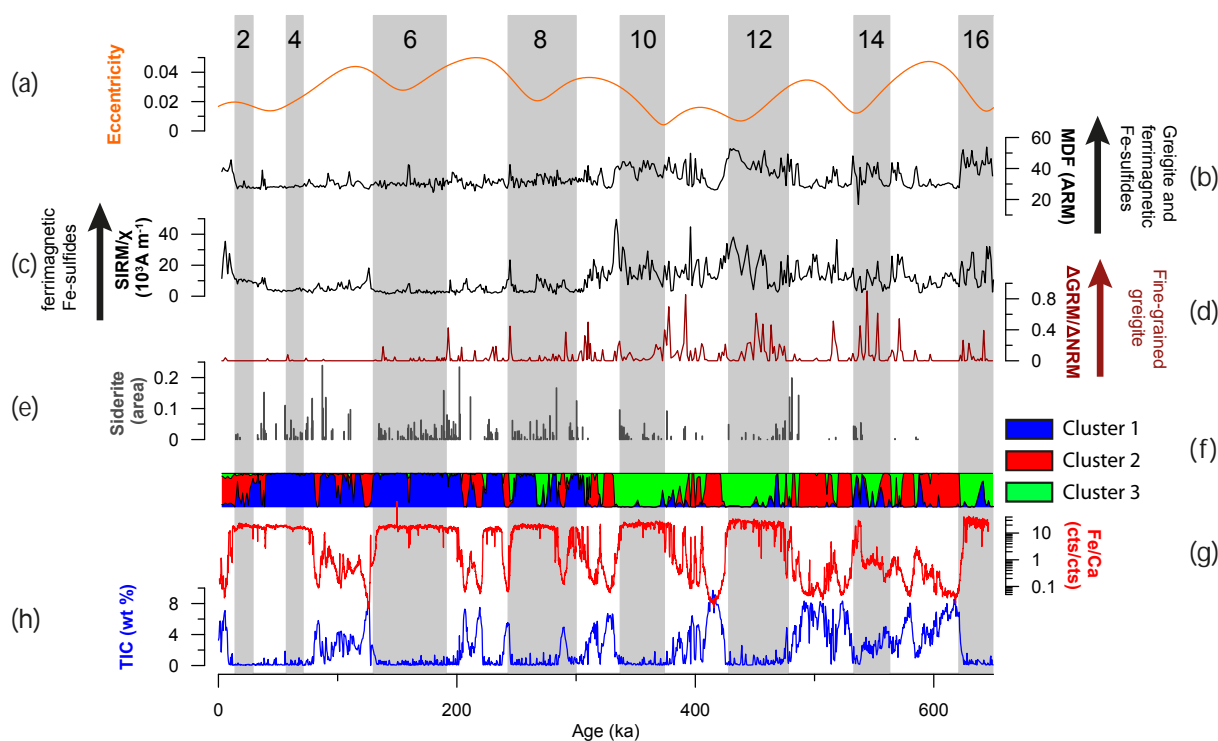


**Figure 5.** Compilation of parameters indicative of early diagenetic Fe-mineral formation, compared to (a) eccentricity (after Laskar et al., 2004).  $MDF_{(ARM)}$  (b),  $SIRM/\chi$  (c) and  $\Delta GRM/\Delta NRM$  (d) are elevated in the lower part, while siderite abundances (e) are higher in the upper part of the core. Cluster-membership coefficients (f) imply a glacial–interglacial pattern for iron sulfides (green). Iron sulfides and siderites occur also at elevated Fe/Ca (g) ratios during interglacials. Geochemical differences between the upper and lower unit are also visible for TIC (h) concentrations during interglacials.

iron reduction is higher than the rate of sulfate reduction (e.g. Pye, 1981, 1990). Sulfate concentrations are much lower in lakes (10–500  $\mu\text{M}$ ), compared to the ocean (28 mM; Holmer and Storkholm, 2001), and sulfate is depleted within the uppermost centimeter of the sediments. Thus, methanogenesis plays a more important role for organic matter degradation compared to marine environments (Capone and Kiene, 1988).

During late diagenesis, iron sulfides may precipitate from mineralized fluids (Sagnotti et al., 2010) if pore-water chemistry changes, i.e., by up- or downward-migrating dissolved  $\text{H}_2\text{S}$  species. Newly formed iron sulfides have been observed to overgrow earlier diagenetic iron minerals, such as siderite (Roberts and Weaver, 2005; Sagnotti et al., 2005).

From SEM observations, we find no indication that sulfides formed at a later stage than siderites. Sulfide nodules are much coarser than the apparently well-preserved siderite crystals (Fig. 3g). The shape of iron sulfide nodules rather appear to fill cavities of former organic compounds (Fig. 3c).

Siderite abundances are higher in the upper part of the core (Fig. 5e), where the ferrimagnetic iron sulfide proxies are low. In the older glacials of unit 2, siderite concentrations decrease when GRM,  $MDF_{ARM}$  and/or  $SIRM/\chi$  increases (Fig. 5b–d). This rather suggests that during early diagenesis

one over the other, iron sulfide or siderite formation dominated.

Finally, this assumption is supported by unpublished relative paleointensity (RPI) data that will be presented elsewhere. If the ferrimagnetic iron sulfides formed later during diagenesis, a disruption of the match between the RPI trend from Lake Ohrid and global RPI stacks would be expected. However, the good quality of the RPI correlation suggests that the iron sulfide nodules, associated with elevated  $SIRM/\chi$ , grew during early diagenesis.

### 5.5 Large-scale shifts in redox conditions

The most prominent feature of the magnetic record is the transition from a dominance of iron sulfides in unit 2 (> 320 ka) and siderite in unit 1 (< 320 ka), suggesting a change in pore-water chemistry. Other proxy data sets from the Ohrid composite profile also indicate that lacustrine conditions changed at this boundary. As outlined above, siderite abundances are distinctly higher in the upper part of the core (Fig. 5e). Furthermore, interglacial TIC concentrations are generally lower in the upper unit 1 (up to 6%) compared to unit 2 (up to 10%, Fig. 5h), while interglacial TOC concentrations are relatively low in unit 2 (Fig. 2l). The higher concentrations of TIC relative to TOC were tentatively dis-

cussed to be dependent on higher ion concentrations in lake water due to increased evaporation (Lacey et al., 2016) during the deposition of the lower unit, but could also relate to enhanced organic matter degradation (Francke et al., 2015).

As outlined above, siderite typically forms during methanogenesis (Berner, 1981), which is the only process for organic matter degradation after sulfate is consumed. The shift of siderite to sulfide formation implies a shift in the redox conditions between unit 1 and 2. We propose that, during the deposition of unit 1,  $\text{SO}_4$  was rapidly consumed in the shallow sediments, or even within the bottom water. Magnetic iron oxides were readily reduced, but due to the lack of sufficient  $\text{H}_2\text{S}$ , siderite precipitated out of  $\text{CaCO}_3$  supersaturated waters (Coleman et al., 1985), as was also observed in the sister lake Prespa (Leng et al., 2013). In contrast, the sulfidic zone apparently penetrated deeper into the sediments during the deposition of unit 2. Pyrite formation (Canfield and Berner, 1987) and, thus, precursors of pyrite, such as greigite, require sulfate concentrations  $> 1$  mM. These prerequisites were apparently met; however, sulfate concentrations were probably still low, and not sufficient to transform metastable iron sulfides into pyrite.

The depth of the sulfidic zone is influenced by a number of different processes which can modulate each other. First of all, the input of sulfate or sulfide could differ. Generally, sulfate is mainly derived from sulfur-bearing weathered rocks in the catchment (Holmer and Storkholm, 2001). Enhanced erosion or a stronger chemical weathering could thus increase the sulfate supply to the lake. Sulfides may also derive from upward-migrating fluids in active tectonic settings. Secondly, even if sulfate fluxes are stable, sulfate concentrations increase when evaporation is enhanced. Another process of sulfate consumption in the sediments is linked to  $\text{O}_2$  concentrations in the bottom water and to the accumulation and degradation of organic matter. Enhanced degradation of organic matter within the oxic zone, e.g., due to better ventilation of bottom water, would modify the oxidation state of bottom water and shift the sulfidic zone to a deeper depth.

At this point we cannot infer which process, or combination of processes, is responsible for the observed pattern. Given that Lake Ohrid is a subsiding basin, the water volume of the lake may have been smaller during deposition of unit 2. This could have led to a more regular deep mixing of Lake Ohrid and a slower sulfate consumption, both resulting in the sulfidic zone migrating deeper into the underlying sediments. This scenario is in line with higher TIC concentrations in the lower part of the core most likely due to higher ion concentrations and to comparably low TOC concentrations, linked to organic matter degradation. In addition, the glacials in the lower part of the core correspond to phases of low eccentricity, i.e., weaker seasonality (Fig. 5a). The annual temperature distribution may have had an additional effect on deep convection and lacustrine productivity of Lake Ohrid, which might have contributed to a change in mixing processes and the production and degradation of organic material.

## 5.6 Glacial–interglacial variability of iron sulfide formation

Ferrimagnetic iron sulfides (paramagnetic siderites) are contained within glacial sediments in the lower (upper) unit. Moreover, diagenetic Fe minerals, represented by the iron sulfide cluster (Fig. 5f) and siderite abundances (Fig. 5e), occur at peak Fe / Ca ratios and minimum TIC concentrations (Fig. 5) within interglacials.

In the older glacials (unit 2), siderite concentrations are high when GRM acquisition and  $\text{SIRM} / \chi$  is relatively low, and vice versa.  $\text{SIRM} / \chi$  rises, in turn, to maximum values when GRM and siderite content are reduced. Again, this highlights the importance of sulfate concentrations and Fe availability for the early diagenetic formation of iron minerals.

A further characterization of iron-mineral genesis in the course of redox conditions, however, needs to be further investigated by performing geochemical and mineralogical classification. Sulfur isotopes could further improve the understanding of the sulfur source, and a discrimination of the chemical composition of the iron sulfide nodules will help to understand the processes responsible for their formation and preservation.

## 5.7 High-coercivity minerals in Lake Ohrid sediments

Since the magnetic signal in unit 2 is dominated by the presence of diagenetic ferrimagnetic iron sulfides, we only investigated unit 1 (MIS 1–MIS 8) for changing lithogenic sediment supply (Fig. 5). Terrigenous input vs. limnic productivity is high during glacials, indicated by higher Fe / Ca ratio, and higher susceptibility (integrating ferri- and paramagnetic minerals) and low TIC concentrations. At the same time, the concentration of high-coercivity magnetic minerals increases within the magnetic fraction (indicated by the  $S$  ratio). Since this pattern is not due to preferential dissolution of magnetite (cf. Sect. 5.1), we propose that the composition of terrigenous input changed over glacial–interglacial timescales.

The catchment of Lake Ohrid comprises different lithologies (cf. Sect. 1) that are mirrored by the distribution of element concentrations in surface sediments (Vogel et al., 2010b). Vogel et al. (2010a) assumed that changes in Cr / Ti ratios on glacial–interglacial timescales result from either increased aeolian activity or a stronger erosion of soil material from sparsely vegetated soils. The detrital iron oxides in the magnetic extracts often contain Cr, which is a typical element for mantle rocks. The ophiolite belt, located west of the basin, is therefore a possible source for the magnetic minerals in Lake Ohrid. The magnetic mineralogy of the ophiolites (oceanic core complexes) in the Albanides consists mainly of magnetite (Maffione et al., 2014).

We observe a large similarity between the benthic  $\delta^{18}\text{O}$  stack (Lisiecki and Raymo, 2005) and the  $S$  ratio from Lake Ohrid (Fig. 3b, c). This suggests compositional changes

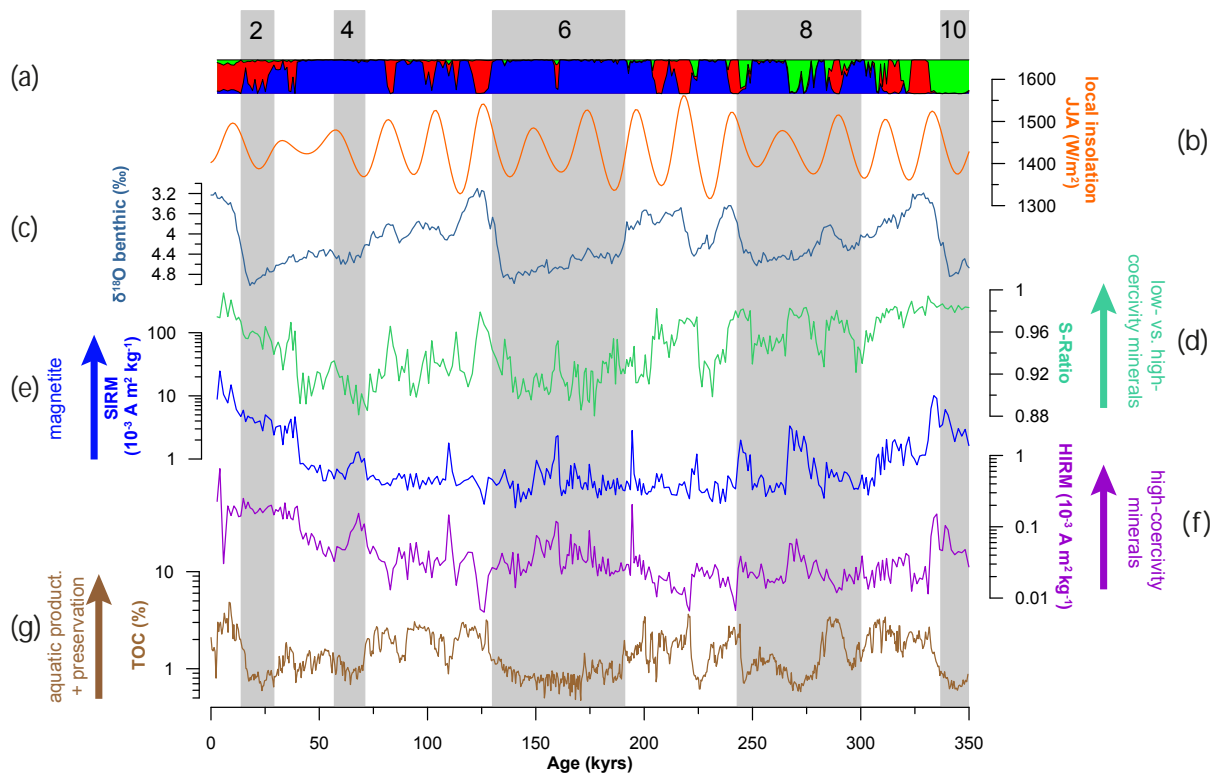


**Figure 6.** Cluster-membership coefficients (a), rock-magnetic properties (d–f) and TOC concentration (g) for unit 1 compared to (a) summer insolation at Lake Ohrid (after Laskar et al., 2004) and (b) benthic  $\delta^{18}\text{O}$  stack (Lisiecki and Raymo, 2005). Changing magnetic mineralogy parallels glacial–interglacial variability and summer insolation.

in the magnetic mineralogy reflect changing environmental conditions. During warm (and humid) interglacials, chemical weathering was enhanced and accumulation of soils and pedogenetic formation of (magnetic) minerals was promoted. However, as already proposed by Vogel et al. (2010a), vegetation cover prevented the erosion of the soil materials, and terrigenous magnetic minerals were diluted by biogenic sedimentary components. In the following glacials, vegetation cover decreased, as is indicated by arboreal pollen abundances from Lake Ohrid (Sadori et al., 2015) and soils were exposed and more susceptible to erosion. As a result, increased input of high-coercivity minerals, e.g., hematite and/or goethite, can be observed, the latter being the most widespread pedogenetic magnetic minerals (Cornell and Schwertmann, 2006; Vodyanitskii, 2010).

During interglacials, the  $S$  ratio (Fig. 6d) and  $\chi_{\text{ARM}}/\text{SIRM}$  (cf. Fig. 2g) show higher frequency variations, where low values approximate to local summer insolation minima (Fig. 6b). Offsets, e.g., during MIS 5, might be related to age uncertainties ( $\pm 2000$  years for the Lake Ohrid record; Francke et al., 2015). Changes in the magnetic mineralogy in concert with insolation are also mirrored by the cluster membership coefficients (Fig. 6a). Similar to the mechanism proposed above, these low-insolation phases correspond to relatively cold condi-

tions and less dense vegetation cover, also visible in pollen abundance patterns (Sadori et al., 2015), thus increasing erosion of soil materials.

### 5.8 Bacterial magnetite in Lake Ohrid sediments?

In the uppermost 6 m of the core, covering the Holocene,  $\chi_{\text{ARM}}/\text{SIRM}$  and  $\text{SIRM}$  and  $\text{SIRM}/\chi$  reach the highest values of the sequence (Fig. 2). An increased input of lithogenic magnetic minerals relative to carbonates can be ruled out since TOC and TIC concentrations are high (Figs. 2 and 4).

One source for magnetic minerals, independent of detrital material supply, is the production of bacterial magnetite and greigite. Magnetotactic bacteria utilize dissolved iron that is available either in the water column or at the  $\text{Fe}^{2+}$ – $\text{Fe}^{3+}$  redox boundary in the sediment (Kopp and Kirschvink, 2008). These bacteria produce magnetite (Blakemore, 1975; Frankel et al., 1979) or greigite (Heywood et al., 1990; Mann et al., 1990) crystals, so-called magnetosomes, within or outside their cells. It was shown that production of bacterial magnetite is linked to increasing organic matter supply (Egli, 2004a; Roberts et al., 2011b; Snowball et al., 2002), at least for oxic lakes (Egli, 2004b). Moreover, the production of bacterial magnetite can be fostered by the input of nutri-

ents (Egli, 2004b). Magnetotactic bacteria producing greigite prefer reducing conditions, and greigite magnetosomes have a higher potential for preservation under sulfidic conditions (Chang et al., 2014; Vasiliev et al., 2008). Fine magnetite crystals have a potential for preservation if certain environmental conditions, e.g., supply of oxygen and concentration of hydrogen sulfide, are met (Canfield and Berner, 1987). In Fig. 3, the Holocene samples are the only ones that coincide with the area of bacterial magnetite and greigite. The concurrence of elevated TOC together with the fine-grained magnetic phase could therefore indicate the presence of bacterial magnetite. However, we cannot infer whether this occurrence is triggered by high TOC and/or nutrient input, or whether it results from a not-yet-completed dissolution of magnetosomes (Snowball, 1994).

## 6 Conclusions

Rock-magnetic data, in conjunction with sedimentological and geochemical data from the Lake Ohrid DEEP site, signify changing terrestrial climate conditions, as well as changes in the lacustrine system over the past 637 kyr. Magnetic parameters often associated with greigite are elevated in glacial periods in the lower part of the core (637–320 ka, unit 2). SEM investigations support the presence of greigite and/or other iron sulfides. Ferrimagnetic iron sulfides are absent in the upper part of the core (0–320 ka, unit 1), where instead siderite is abundant in glacial sediments. Siderite typically forms during methanogenesis after  $\text{SO}_4$  is consumed, we propose that a geochemical shift occurred in Lake Ohrid with higher (lower) sulfate availability during the deposition of the lower (upper) unit. Various mechanisms might be responsible for this pattern. However, based on higher TIC concentrations within the interglacial periods of the lower unit, which are probably linked to higher ion concentrations in the lake water, we suggest that sulfate flux was enhanced and/or sulfate was concentrated due to a smaller water volume or enhanced evaporation. Further studies on the iron sulfide mineralogy and sulfur isotopes are required to provide a better understanding of the sources of sulfur and processes responsible for differences in Fe-S morphology and chemistry.

The magnetic properties of sediments deposited during the past 320 kyr are also observed to signify changes in terrestrial environmental conditions on glacial and interglacial timescales. During glacials, high-coercivity magnetic minerals (e.g., hematite and goethite) that formed in the course of pedogenesis in preceding interglacials were deposited in the lake. In contrast, a rich catchment vegetation during interglacials limited the erosion of soil material and only minor detrital magnetite originating from physically weathered rocks was transported into Lake Ohrid. Millennial-scale variations in rock-magnetic properties, which are concurrent with changes in summer insolation, suggest that the proposed

mechanism of vegetation expansion also influenced the erosion of soil materials on shorter timescales. Magnetic concentration parameters in the Holocene (upper 6 m) are enhanced, while carbonate and TOC concentrations, normally diluting the magnetic signal, are also high. Together with magnetic proxies for magnetic coercivity, these samples are suspected to contain bacterial magnetite. Overall, our findings demonstrate the valuable contribution of rock-magnetic methods to environmental studies, as they provide important information about a suite of different processes, comprising studies on terrestrial environmental conditions, sediment dynamics and internal lake processes.

## Data availability

All rock-magnetic data are available from PANGAEA (Just et al., 2015) at doi:10.1594/PANGAEA.848639. Geochemical data are from Francke et al. (2016) and siderite data are from Lacey et al. (2016).

*Acknowledgements.* The SCOPSCO Lake Ohrid drilling campaign was funded by the ICDP, the German Ministry of Higher Education and Research, the German Research Foundation, the University of Cologne, the British Geological Survey, the INGV and CNR (both Italy), and the governments of the republics of Macedonia (FYROM) and Albania. Logistic support was provided by the Hydrobiological Institute in Ohrid. Drilling was carried out by Drilling, Observation and Sampling of the Earth's Continental Crust (DOSECC) and using the Deep Lake Drilling System (DLDS). Special thanks to Beau Marshall and the drilling team. Ali Skinner and Martin Melles provided immense help and advice during logistic preparation and the drilling operation. We acknowledge many student assistants for sediment sampling. We also thank the two anonymous reviewers for constructive feedback on the manuscript. J. Just was financially supported through the Collaborative Research Centre 806, Deutsche Forschungsgemeinschaft.

Edited by: T. Wilke

## References

- Baumgarten, H., Wonik, T., Tanner, D. C., Francke, A., Wagner, B., Zanchetta, G., Sulpizio, R., Giaccio, B., and Nomade, S.: Age-depth model of the past 630 kyr for Lake Ohrid (FYROM/Albania) based on cyclostratigraphic analysis of downhole gamma ray data, *Biogeosciences*, 12, 7453–7465, doi:10.5194/bg-12-7453-2015, 2015.
- Bell, P. E., Mills, A. L., and Herman, J. S.: Biogeochemical Conditions Favoring Magnetite Formation during Anaerobic Iron Reduction, *Appl. Environ. Microbiol.*, 53, 2610–2616, 1987.
- Berner, R. A.: A new geochemical classification of sedimentary environments, *J. Sediment. Res.*, 51, 351–369, 1981.
- Blakemore, R.: Magnetotactic bacteria, *Science*, 190, 377–379, 1975.

- Blanchet, C., Thouveny, N., and Vidal, L.: Formation and preservation of greigite ( $\text{Fe}_3\text{S}_4$ ) in sediments from the Santa Barbara Basin: Implications for paleoenvironmental changes during the past 35 ka, *Paleoceanography*, 24, PA2224, doi:10.1029/2008PA001719, 2009.
- Canfield, D. E. and Berner, R. A.: Dissolution and pyritization of magnetite in anoxic marine sediments, *Geochim. Cosmochim. Ac.*, 51, 645–659, 1987.
- Capone, D. G. and Kiene, R. P.: Comparison of microbial dynamics in marine and freshwater sediments: Contrasts in anaerobic carbon catabolism, *Limnol. Oceanogr.*, 33, 725–749, 1988.
- Chang, L., Vasiliev, I., van Baak, C., Krijgsman, W., Dekkers, M. J., Roberts, A. P., Fitz Gerald, J. D., van Hoesel, A., and Winklhofer, M.: Identification and environmental interpretation of diagenetic and biogenic greigite in sediments: A lesson from the Messinian Black Sea, *Geochem. Geophys. Geosy.*, 15, 3612–3627, 2014.
- Coleman, M. L., Berner, R. A., Durand, B., Meadows, P. S., and Eglinton, G.: Geochemistry of Diagenetic Non-Silicate Minerals Kinetic Considerations [and Discussion], *Philos. T. Roy. Soc. A*, 315, 39–56, 1985.
- Cornell, R. M. and Schwertmann, U.: The iron oxides: structure, properties, reactions, occurrence and uses, John Wiley & Sons, 2006.
- DeMenocal, P., Bloemendal, J., and King, J.: A rock-magnetic record of monsoonal dust deposition to the Arabian Sea: evidence for a shift in the mode of deposition at 2.4 Ma, *Proceed. ODP, Sci. Results*, 117, 389–407, 1991.
- Demory, F., Oberhänsli, H., Nowaczyk, N. R., Gottschalk, M., Wirth, R., and Naumann, R.: Detrital input and early diagenesis in sediments from Lake Baikal revealed by rock magnetism, *Global Planet. Change*, 46, 145–166, 2005.
- Dong, H., Fredrickson, J. K., Kennedy, D. W., Zachara, J. M., Kukkadapu, R. K., and Onstott, T. C.: Mineral transformations associated with the microbial reduction of magnetite, *Chem. Geol.*, 169, 299–318, 2000.
- Egli, R.: Characterization of individual rock magnetic components by analysis of remanence curves, 1. Unmixing natural sediments, *Stud. Geophys. Geod.*, 48, 391–446, 2004a.
- Egli, R.: Characterization of individual rock magnetic components by analysis of remanence curves. 3. Bacterial magnetite and natural processes in lakes, *Phys. Chem. Earth*, 29, 869–884, 2004b.
- Francke, A., Wagner, B., Just, J., Leicher, N., Gromig, R., Baumgarten, H., Vogel, H., Lacey, J. H., Sadori, L., Wonik, T., Leng, M. J., Zanchetta, G., Sulpizio, R., and Giaccio, B.: Sedimentological processes and environmental variability at Lake Ohrid (Macedonia, Albania) between 637 ka and the present, *Biogeosciences*, 13, 1179–1196, doi:10.5194/bg-13-1179-2016, 2016.
- Frank, U., Nowaczyk, N. R., Minyuk, P., Vogel, H., Rosén, P., and Melles, M.: A 350 ka record of climate change from Lake El'gygytgyn, Far East Russian Arctic: refining the pattern of climate modes by means of cluster analysis, *Clim. Past*, 9, 1559–1569, doi:10.5194/cp-9-1559-2013, 2013.
- Frank, U., Nowaczyk, N. R., and Negendank, J. F. W.: Rock magnetism of greigite bearing sediments from the Dead Sea, Israel, *Geophys. J. Int.*, 168, 921–934, 2007.
- Frank, U., Nowaczyk, N. R., Negendank, J. F. W., and Melles, M.: A paleomagnetic record from Lake Lama, northern Central Siberia, *Phys. Earth Planet. In.*, 133, 3–20, 2002.
- Frankel, R. B. and Bazylinski, D. A.: Biologically Induced Mineralization by Bacteria, *Rev. Mineral. Geochem.* 54, 95–114, 2003.
- Frankel, R. B., Blakemore, R. P., and Wolfe, R. S.: Magnetite in Freshwater Magnetotactic Bacteria, *Science*, 203, 1355–1356, 1979.
- Froelich, P. N., Klinkhammer, G. P., Bender, M. L., Luedtke, N. A., Heath, G. R., Cullen, D., Dauphin, P., Hammond, D., Hartman, B., and Maynard, V.: Early oxidation of organic matter in pelagic sediments of the eastern equatorial Atlantic: suboxic diagenesis, *Geochim. Cosmochim. Ac.*, 43, 1075–1090, 1979.
- Fu, C., Bloemendal, J., Qiang, X., Hill, M. J., and An, Z.: Occurrence of greigite in the Pliocene sediments of Lake Qinghai, China, and its paleoenvironmental and paleomagnetic implications, *Geochem. Geophys. Geosy.*, 1293–1306, doi:10.1002/2014GC005677, 2015.
- Fu, Y., von Dobeneck, T., Franke, C., Heslop, D., and Kasten, S.: Rock magnetic identification and geochemical process models of greigite formation in Quaternary marine sediments from the Gulf of Mexico (IODP Hole U1319A), *Earth Planet. Sc. Lett.*, 275, 233–245, 2008.
- Heywood, B. R., Bazylinski, D. A., Garratt-Reed, A., Mann, S., and Frankel, R. B.: Controlled biosynthesis of greigite ( $\text{Fe}_3\text{S}_4$ ) in magnetotactic bacteria, *Naturwissenschaften*, 77, 536–538, 1990.
- Hoffmann, N., Reicherter, K., Fernández-Steege, T., and Grützner, C.: Evolution of ancient Lake Ohrid: a tectonic perspective, *Biogeosciences*, 7, 3377–3386, doi:10.5194/bg-7-3377-2010, 2010.
- Holmer, M. and Storkholm, P.: Sulphate reduction and sulphur cycling in lake sediments: a review, *Freshwater Biol.*, 46, 431–451, 2001.
- Hounslow, M. W. and Maher, B. A.: Source of the climate signal recorded by magnetic susceptibility variations in Indian Ocean sediments, *J. Geophys. Res.-Sol. Ea.*, 104, 5047–5061, 1999.
- Hu, P., Liu, Q., Heslop, D., Roberts, A. P., and Jin, C.: Soil moisture balance and magnetic enhancement in loess–paleosol sequences from the Tibetan Plateau and Chinese Loess Plateau, *Earth Planet. Sc. Lett.*, 409, 120–132, 2015.
- Just, J., Heslop, D., von Dobeneck, T., Bickert, T., Dekkers, M. J., Frederichs, T., Meyer, I., and Zabel, M.: Multiproxy characterization and budgeting of terrigenous end-members at the NW African continental margin, *Geochem. Geophys. Geosy.*, 13, Q0A001, doi:10.1029/2012gc004148, 2012.
- Just, J., Nowaczyk, N. R., Sagnotti, L., Francke, A., Vogel, H., Lacey, J., and Wagner, B.: Rock-magnetic properties of ICDP core 5045-1 (640 ka), Lake Ohrid, doi:10.1594/PANGAEA.848639, 2015.
- Kämpf, N. and Schwertmann, U.: Goethite and hematite in a climosequence in southern Brazil and their application in classification of kaolinitic soils, *Geoderma*, 29, 27–39, 1983.
- Kao, S.-J., Horng, C.-S., Roberts, A. P., and Liu, K.-K.: Carbon–sulfur–iron relationships in sedimentary rocks from southwestern Taiwan: influence of geochemical environment on greigite and pyrrhotite formation, *Chem. Geol.*, 203, 153–168, 2004.
- Karlin, R. and Levi, S.: Diagenesis of magnetic minerals in recent haemipelagic sediments, *Nature*, 303, 327–330, 1983.
- Kasten, S., Freudenthal, T., Gingele, F. X., and Schulz, H. D.: Simultaneous formation of iron-rich layers at different redox boundaries in sediments of the Amazon deep-sea fan, *Geochim. Cosmochim. Ac.*, 62, 2253–2264, 1998.

- King, J., Banerjee, S. K., Marvin, J., and Özdemir, Ö.: A comparison of different magnetic methods for determining the relative grain size of magnetite in natural materials: Some results from lake sediments, *Earth Planet. Sc. Lett.*, 59, 404–419, 1982.
- Kopp, R. E. and Kirschvink, J. L.: The identification and biogeochemical interpretation of fossil magnetotactic bacteria, *Earth-Sci. Rev.*, 86, 42–61, 2008.
- Lacey, J. H., Leng, M. J., Francke, A., Sloane, H. J., Milodowski, A., Vogel, H., Baumgarten, H., Zanchetta, G., and Wagner, B.: Northern Mediterranean climate since the Middle Pleistocene: a 637 ka stable isotope record from Lake Ohrid (Albania/Macedonia), *Biogeosciences*, 13, 1801–1820, doi:10.5194/bg-13-1801-2016, 2016.
- Larrasoña, J. C., Roberts, A. P., Liu, Q., Lyons, R., Oldfield, F., Rohling, E. J., and Heslop, D.: Source-to-sink magnetic properties of NE Saharan dust in Eastern Mediterranean marine sediments: a review and paleoenvironmental implications, *Front. Earth Sci.*, 3, doi:10.3389/feart.2015.00019, 2015.
- Laskar, J., Robutel, P., Joutel, F., Gastineau, M., Correia, A., and Levrard, B.: A long-term numerical solution for the insolation quantities of the Earth, *Astron. Astrophys.*, 428, 261–285, 2004.
- Leicher, N., Zanchetta, G., Sulpizio, R., Giaccio, B., Wagner, B., Nomade, S., Francke, A., and Del Carlo, P.: First tephrostratigraphic results of the DEEP site record from Lake Ohrid, Macedonia, *Biogeosciences Discuss.*, 12, 15411–15460, doi:10.5194/bgd-12-15411-2015, 2015.
- Leng, M. J., Wagner, B., Boehm, A., Panagiotopoulos, K., Vane, C. H., Snelling, A., Haidon, C., Woodley, E., Vogel, H., Zanchetta, G., and Banerjee, I.: Understanding past climatic and hydrological variability in the Mediterranean from Lake Prespa sediment isotope and geochemical record over the Last Glacial cycle, *Quaternary Sci. Rev.*, 66, 123–136, 2013.
- Lézine, A. M., von Grafenstein, U., Andersen, N., Belmecheri, S., Bordon, A., Caron, B., Cazet, J. P., Erlenkeuser, H., Fouache, E., Grenier, C., Huntsman-Mapila, P., Hureau-Mazaudier, D., Manelli, D., Mazaud, A., Robert, C., Sulpizio, R., Tiercelin, J. J., Zanchetta, G., and Zeqollari, Z.: Lake Ohrid, Albania, provides an exceptional multi-proxy record of environmental changes during the last glacial-interglacial cycle, *Palaeogeogr. Palaeoecol.*, 287, 116–127, 2010.
- Lisiecki, L. E. and Raymo, M. E.: A Pliocene-Pleistocene stack of 57 globally distributed benthic  $\delta^{18}\text{O}$  records, *Paleoceanography*, 20, PA1003, doi:10.1029/2004PA001071, 2005.
- Lyons, R., Oldfield, F., and Williams, E.: Mineral magnetic properties of surface soils and sands across four North African transects and links to climatic gradients, *Geochem. Geophys. Geos.*, 11, Q08023, doi:10.1029/2010gc003183, 2010.
- Maffione, M., Morris, A., Plümpner, O., and van Hinsbergen, D. J. J.: Magnetic properties of variably serpentinized peridotites and their implication for the evolution of oceanic core complexes, *Geochem. Geophys. Geos.*, 15, 923–944, 2014.
- Maher, B. A.: The magnetic properties of Quaternary aeolian dusts and sediments, and their palaeoclimatic significance, *Aeolian Res.*, 3, 87–144, 2011.
- Maher, B. A. and Thompson, R.: Paleoclimatic significance of the mineral magnetic record of the Chinese loess and paleosols, *Quaternary Res.*, 37, 155–170, 1992.
- Maher, B. A. and Thompson, R.: Quaternary climates, environments and magnetism, Cambridge University Press, 1999.
- Mann, S., Sparks, N. H. C., Frankel, R. B., Bazylinski, D. A., and Jannasch, H. W.: Biomineralization of ferrimagnetic greigite ( $\text{Fe}_3\text{S}_4$ ) and iron pyrite ( $\text{FeS}_2$ ) in a magnetotactic bacterium, *Nature*, 343, 258–261, 1990.
- Matzinger, A., Jordanoski, M., Veljanoska-Sarafiloska, E., Sturm, M., Müller, B., and Wüest, A.: Is Lake Prespa Jeopardizing the Ecosystem of Ancient Lake Ohrid?, *Hydrobiologia*, 553, 89–109, 2006a.
- Matzinger, A., Spirkovski, Z., Patceva, S., and Wüest, A.: Sensitivity of Ancient Lake Ohrid to Local Anthropogenic Impacts and Global Warming, *J. Great Lakes Res.*, 32, 158–179, 2006b.
- Matzinger, A., Schmid, M., Veljanoska-Sarafiloska, E., Patceva, S., Guseska, D., Wagner, B., Müller, B., Sturm, M., and Wüest, A.: Eutrophication of ancient Lake Ohrid: Global warming amplifies detrimental effects of increased nutrient inputs, *Limnol. Oceanogr.*, 52, 338–353, 2007.
- Nowaczyk, N. R.: Dissolution of titanomagnetite and sulphidization in sediments from Lake Kinneret, Israel, *Geophys. J. Int.*, 187, 34–44, 2011.
- Nowaczyk, N. R., Arz, H. W., Frank, U., Kind, J., and Plessen, B.: Dynamics of the Laschamp geomagnetic excursion from Black Sea sediments, *Earth Planet. Sc. Lett.*, 351–352, 54–69, 2012.
- Nowaczyk, N. R., Haltia, E. M., Ulbricht, D., Wennrich, V., Sauerbrey, M. A., Rosén, P., Vogel, H., Francke, A., Meyer-Jacob, C., Andreev, A. A., and Lozhkin, A. V.: Chronology of Lake El'gygytgyn sediments – a combined magnetostratigraphic, palaeoclimatic and orbital tuning study based on multiparameter analyses, *Clim. Past*, 9, 2413–2432, doi:10.5194/cp-9-2413-2013, 2013.
- Nowaczyk, N. R., Minyuk, P., Melles, M., Brigham-Grette, J., Glushkova, O., Nolan, M., Lozhkin, A. V., Stetsenko, T. V., M. Andersen, P., and Forman, S. L.: Magnetostratigraphic results from impact crater Lake El'gygytgyn, northeastern Siberia: a 300 kyr long high-resolution terrestrial palaeoclimatic record from the Arctic, *Geophys. J. Int.*, 150, 109–126, 2002.
- Peck, J. A., Green, R. R., Shanahan, T., King, J. W., Overpeck, J. T., and Scholz, C. A.: A magnetic mineral record of Late Quaternary tropical climate variability from Lake Bosumtwi, Ghana, *Palaeogeogr. Palaeoecol.*, 215, 37–57, 2004.
- Peck, J. A., King, J. W., Colman, S. M., and Kravchinsky, V. A.: A rock-magnetic record from Lake Baikal, Siberia: Evidence for Late Quaternary climate change, *Earth Planet. Sc. Lett.*, 122, 221–238, 1994.
- Peters, C. and Dekkers, M. J.: Selected room temperature magnetic parameters as a function of mineralogy, concentration and grain size, *Phys. Chem. Earth, Parts A/B/C*, 28, 659–667, 2003.
- Popovska, C. and Bonacci, O.: Basic data on the hydrology of Lakes Ohrid and Prespa, *Hydrol. Process.*, 21, 658–664, 2007.
- Pye, K.: Marshrock formed by iron sulphide and siderite cementation in saltmarsh sediments, *Nature*, 294, 650–652, 1981.
- Pye, K., Dickson, J. A. D., Schiavon, N., Coleman, M. L., and Cox, M.: Formation of siderite-Mg-calcite-iron sulphide concretions in intertidal marsh and sandflat sediments, north Norfolk, England, *Sedimentology*, 37, 325–343, doi:10.1111/j.1365-3091.1990.tb00962.x, 1990.
- Reinholdsson, M., Snowball, I., Zillén, L., Lenz, C., and Conley, D. J.: Magnetic enhancement of Baltic Sea sapropels by greigite magnetofossils, *Earth Planet. Sc. Lett.*, 366, 137–150, 2013.

- Reynolds, R. L. and King, J. W.: Magnetic records of climate change, *Rev. Geophys.*, 33, 101–110, 1995.
- Roberts, A. P.: Magnetic mineral diagenesis, *Earth-Sci. Rev.*, 151, 1–47, 2015.
- Roberts, A. P., Chang, L., Heslop, D., Florindo, F., and Larrasoana, J. C.: Searching for single domain magnetite in the “pseudo-single-domain” sedimentary haystack: Implications of biogenic magnetite preservation for sediment magnetism and relative paleointensity determinations, *J. Geophys. Res.-Sol. Ea.*, 117, B08104, doi:10.1029/2012JB009412, 2012.
- Roberts, A. P., Chang, L., Rowan, C. J., Horng, C.-S., and Florindo, F.: Magnetic properties of sedimentary greigite (Fe<sub>3</sub>S<sub>4</sub>): An update, *Rev. Geophys.*, 49, RG1002, doi:10.1029/2010RG000336, 2011a.
- Roberts, A. P., Florindo, F., Villa, G., Chang, L., Jovane, L., Bohaty, S. M., Larrasoana, J. C., Heslop, D., and Fitz Gerald, J. D.: Magnetotactic bacterial abundance in pelagic marine environments is limited by organic carbon flux and availability of dissolved iron, *Earth Planet. Sc. Lett.*, 310, 441–452, 2011b.
- Roberts, A. P., Reynolds, R. L., Verosub, K. L., and Adam, D. P.: Environmental magnetic implications of Greigite (Fe<sub>3</sub>S<sub>4</sub>) Formation in a 3 m.y. lake sediment record from Butte Valley, northern California, *Geophys. Res. Lett.*, 23, 2859–2862, 1996.
- Roberts, A. P. and Weaver, R.: Multiple mechanisms of remagnetization involving sedimentary greigite (Fe<sub>3</sub>S<sub>4</sub>), *Earth Planet. Sc. Lett.*, 231, 263–277, 2005.
- Roberts, A. P., Wilson, G. S., Florindo, F., Sagnotti, L., Verosub, K. L., and Harwood, D. M.: Magnetostratigraphy of lower Miocene strata from the CRP-1 core, McMurdo Sound, Ross Sea, Antarctica, *Terra Antarctica*, 5, 703–713, 1998.
- Ron, H., Nowaczyk, N. R., Frank, U., Schwab, M. J., Naumann, R., Striewski, B., and Agnon, A.: Greigite detected as dominating remanence carrier in Late Pleistocene sediments, Lisan formation, from Lake Kinneret (Sea of Galilee), Israel, *Geophys. J. Int.*, 170, 117–131, 2007.
- Rowan, C. J., Roberts, A. P., and Broadbent, T.: Reductive diagenesis, magnetite dissolution, greigite growth and paleomagnetic smoothing in marine sediments: A new view, *Earth Planet. Sc. Lett.*, 277, 223–235, 2009.
- Sadori, L., Koutsodendris, A., Masi, A., Bertini, A., Combourieu-Nebout, N., Francke, A., Kouli, K., Joannin, S., Mercuri, A. M., Panagiotopoulos, K., Peyron, O., Torri, P., Wagner, B., Zanchetta, G., and Donders, T. H.: Pollen-based paleoenvironmental and paleoclimatic change at Lake Ohrid (SE Europe) during the past 500 ka, *Biogeosciences Discuss.*, accepted, 12, 15461–15493, doi:10.5194/bgd-12-15461-2015, 2015.
- Sagnotti, L.: Iron Sulfides, in: *Encyclopedia of Geomagnetism and Paleomagnetism*, edited by: Gubbins, D. and Herrero-Bervera, E., Springer, Dordrecht, the Netherlands, 2007.
- Sagnotti, L., Cascella, A., Ciaranfi, N., Macrì, P., Maiorano, P., Marino, M., and Taddeucci, J.: Rock magnetism and palaeomagnetism of the Montalbano Jonico section (Italy): evidence for late diagenetic growth of greigite and implications for magnetostratigraphy, *Geophys. J. Int.*, 180, 1049–1066, 2010.
- Sagnotti, L., Roberts, A. P., Weaver, R., Verosub, K. L., Florindo, F., Pike, C. R., Clayton, T., and Wilson, G. S.: Apparent magnetic polarity reversals due to remagnetization resulting from late diagenetic growth of greigite from siderite, *Geophys. J. Int.*, 160, 89–100, 2005.
- Skinner, B. J., Grimaldi, F., and Erd, R.: Greigite Thio-Spinel of Iron-New Mineral, *Am. Mineral.*, 49, 543–555, 1964.
- Snowball, I.: Mineral magnetic properties of Holocene lake sediments and soils from the Kårsa valley, Lappland, Sweden, and their relevance to palaeoenvironmental reconstruction, *Terra Nova*, 5, 258–270, 1993.
- Snowball, I., Sandgren, P., and Petterson, G.: The mineral magnetic properties of an annually laminated Holocene lake-sediment sequence in northern Sweden, *Holocene*, 9, 353–362, 1999.
- Snowball, I. and Thompson, R.: A stable chemical remanence in Holocene sediments, *J. Geophys. Res.-Sol. Ea.*, 95, 4471–4479, 1990.
- Snowball, I., Zillén, L., and Sandgren, P.: Bacterial magnetite in Swedish varved lake-sediments: a potential bio-marker of environmental change, *Quaternary Int.*, 88, 13–19, 2002.
- Snowball, I. F.: Bacterial magnetite and the magnetic properties of sediments in a Swedish lake, *Earth Planet. Sc. Lett.*, 126, 129–142, 1994.
- Snowball, I. F.: The detection of single-domain greigite (Fe<sub>3</sub>S<sub>4</sub>) using rotational remanent magnetization (RRM) and the effective gyro field (Bg): mineral magnetic and palaeomagnetic applications, *Geophys. J. Int.*, 130, 704–716, 1997a.
- Snowball, I. F.: Gyroremanent magnetization and the magnetic properties of greigite-bearing clays in southern Sweden, *Geophys. J. Int.*, 129, 624–636, 1997b.
- Vali, H., von Dobeneck, T., Amarantidis, G., Förster, O., Morteani, G., Bachmann, L., and Petersen, N.: Biogenic and lithogenic magnetic minerals in Atlantic and Pacific deep sea sediments and their paleomagnetic significance, *Geol. Rundsch.*, 78, 753–764, 1989.
- Vasiliev, I., Dekkers, M. J., Krijgsman, W., Franke, C., Langereis, C. G., and Mullender, T. A. T.: Early diagenetic greigite as a recorder of the palaeomagnetic signal in Miocene–Pliocene sedimentary rocks of the Carpathian foredeep (Romania), *Geophys. J. Int.*, 171, 613–629, 2007.
- Vasiliev, I., Franke, C., Meeldijk, J. D., Dekkers, M. J., Langereis, C. G., and Krijgsman, W.: Putative greigite magnetofossils from the Pliocene epoch, *Nat. Geosci.*, 1, 782–786, 2008.
- Vodyanitskii, Y. N.: Iron hydroxides in soils: A review of publications, *Eurasian Soil Sci.*, 43, 1244–1254, 2010.
- Vogel, H., Wagner, B., Zanchetta, G., Sulpizio, R., and Rosén, P.: A paleoclimate record with tephrochronological age control for the last glacial-interglacial cycle from Lake Ohrid, Albania and Macedonia, *J. Paleolimnol.*, 44, 295–310, 2010a.
- Vogel, H., Wessels, M., Albrecht, C., Stich, H.-B., and Wagner, B.: Spatial variability of recent sedimentation in Lake Ohrid (Albania/Macedonia), *Biogeosciences*, 7, 3333–3342, doi:10.5194/bg-7-3333-2010, 2010b.
- Wagner, B., Lotter, A., Nowaczyk, N., Reed, J., Schwalb, A., Sulpizio, R., Valsecchi, V., Wessels, M., and Zanchetta, G.: A 40 000-year record of environmental change from ancient Lake Ohrid (Albania and Macedonia), *J. Paleolimnol.*, 41, 407–430, 2009.
- Wagner, B., Vogel, H., Zanchetta, G., and Sulpizio, R.: Environmental change within the Balkan region during the past ca. 50 ka recorded in the sediments from lakes Prespa and Ohrid, *Biogeosciences*, 7, 3187–3198, doi:10.5194/bg-7-3187-2010, 2010.

- Wagner, B., Wilke, T., Krastel, S., Zanchetta, G., Sulpizio, R., Reichert, K., Leng, M. J., Grazhdani, A., Trajanovski, S., Francke, A., Lindhorst, K., Levkov, Z., Cvetkoska, A., Reed, J. M., Zhang, X., Lacey, J. H., Wonik, T., Baumgarten, H., and Vogel, H.: The SCOPSCO drilling project recovers more than 1.2 million years of history from Lake Ohrid, *Sci. Dril.*, 17, 19–29, doi:10.5194/sd-17-19-2014, 2014.
- Wang, H., Holmes, J. A., Street-Perrott, F. A., Waller, M. P., and Perrott, R. A.: Holocene environmental change in the West African Sahel: sedimentological and mineral-magnetic analyses of lake sediments from Jikariya Lake, northeastern Nigeria, *J. Quaternary. Sci.*, 23, 449–460, 2008.